IMEKO
XXI WORLD CONGRESS
PRAGUE 2015

IMEKO XXI World Congress

August 30 – September 4, 2015

Full Papers

www.imeko2015.org

Disclaimer

The organizer takes no responsibility for any of the content stated in the proceedings. All fullpapers (extended abstracts respectively) are published as provided by their authors.

ISBN

Authors:	Collective of authors
Editor:	Assoc. Prof. Jan Holub
Title:	XXI IMEKO WORLD CONGRESS – FULL PAPERS
Issued by:	Czech Technical University in Prague
	Faculty of Electrical Engineering, Department of Measurement
Address:	Technicka 2, 166 07 Prague 6, Czech Republic
Tel.:	+420 224 359 814
Printed:	on-line (pdf) only
Pages:	2279
Issue:	1. (2015)
ISBN:	978-80-01-05793-3

XXI IMEKO World Congress "Measurement in Research and Industry"
August 30 – September 4, 2015, Prague, Czech Republic

EFFECTS OF STRAY CAPACITANCE TO GROUND IN BIPOLAR WATER IMPEDANCE MEASUREMENTS BASED ON CAPACITIVE ELECTRODES

Carles Aliau-Bonet, *Ramon Pallas-Areny*

Universitat Politècnica de Catalunya, BarcelonaTech (UPC), Castelldefels, Spain, ramon.pallas@upc.edu

Abstract – Liquid impedance measurements based on capacitive (or contactless) electrodes overcome electrode polarization problems but are affected by stray capacitance from the material being measured to ground, the same as measurements with direct-contact electrodes. This study shows that the effects of that capacitance depend on the impedance being measured and for bipolar impedance measurements they increase when the ratio between that stray capacitance and electrode capacitance increases.

Keywords: capacitive electrodes, stray capacitance to ground, impedance measurements

1. INTRODUCTION

Impedance measurements with capacitive electrodes avoid electrode-solution interactions [1][2] and can be performed through the walls of insulating tanks, pipes and hermetically closed containers such as sealed ampoules [3]. They have been applied to determining the conductivity of liquids [1][3], monitoring fermentation processes [2], multiphase measurements in large pipes [4] and impedance measurements in small capillaries [5][6]. The impedance of capacitive electrodes is certainly much higher than that of direct-contact electrodes based on electrochemical reactions, but measuring at a high-enough frequency reduces electrode impedance and bipolar impedance measurements that rely on various injection-detection strategies become feasible.

Nevertheless, high-value impedances makes the measurement system susceptible to interference from external electric fields, whatever the injection-detection strategy. That interference can be reduced by suitable electric shields but then the stray capacitance between the material being measured and the shield affects measurement results. When a continuous electric shield is unpractical, the stray capacitance from the material to ground can also lead to anomalous results [4][6].

The effects of stray capacitance to ground in bipolar impedance measurements based on two direct-contact electrodes have already been reported [7], but no similar analysis seems to exist for capacitive electrodes, sometimes termed contactless electrodes although they usually establish mechanical contact with the container of the material being measured. In this paper, we analyse the effects of stray capacitance to ground in contactless bipolar impedance measurements performed with grounded auto-balancing bridges found in commercial impedance analysers that use voltage injection and output current detection.

2. IMPEDANCE MODEL

The lumped-parameter equivalent circuit for bipolar impedance measurements with capacitive electrodes when the measured current is that that has flown through the material is shown in Fig. 1. Capacitive electrodes consist of a metal surface covered by a dielectric material in contact with the material under test (Z_x) hence electrode impedance can in principle be modelled by a capacitance C_e if the electrical resistance of the dielectric material is high enough [2]. Electrode separation is assumed to be large enough for the "air" capacitance C_{hl} between them to be negligible. Z_x can be described by a resistance R_x shunted by a capacitance C_x, which are assumed to be constant inside the frequency range of interest. The characteristic angular frequency of the material is $\omega_c = (R_x C_x)^{-1}$ [3]. If the volume of the measured sample is large enough relative to the dimensions of the measurement setup, the (distributed) stray capacitance C_g from the sample to ground must be accounted for [6][7]. In order to include C_g in the lumped-parameter model in Fig. 1, we use the coefficient α [7].

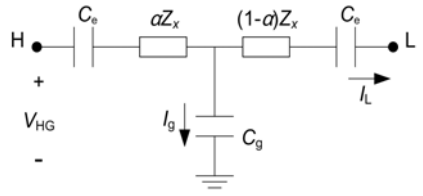

Fig. 1. Three-terminal lumped-parameter model for bipolar impedance measurements with capacitive electrodes.

When Z_x is measured with an earth-grounded commercial impedance analyser based on an auto-balancing bridge that uses the injection-detection strategy in Fig. 1, where terminal L is connected to virtual ground, the actual impedance measured between H and L, if I_g is disregarded, is $Z_{HL} = V_{HG}/I_L = 2/j\omega C_e + Z_x$. Therefore, at low frequencies relative to ω_c we will have $\mathrm{Re}\, Z_{HL} \approx R_x$ and $\mathrm{Im}\, Z_{HL} \approx -2/\omega C_e$, whereas at high frequencies relative to ω_c, Z_{HL} becomes purely capacitive: $Z_{HL} \approx 2/j\omega C_e + 1/j\omega C_x = 1/j\omega C_{HL}$. Nevertheless, if the current through C_g is significant, then current I_L measured by the instrument will be smaller than the actual current provided by the voltage source and the

result will not be $2/j\omega C_e + Z_x$ but a larger impedance which value will increase for increasing frequencies. By applying the delta-star transformation to the circuit in Fig. 1, the measured impedance Z_{HL} when I_g is included will be

$$Z_{HL}(j\omega) = \frac{2 + C_g/C_e}{j\omega C_e} + \frac{R_x}{1 + j\omega R_x C_x}\left(1 + \frac{C_g}{C_e}\right) + \frac{j\omega\alpha(1-\alpha)R_x^2 C_g}{(1 + j\omega R_x C_x)^2} \quad (1)$$

that shows that C_g greatly affects each of the three terms of the result. The first term is due to the impedance of the electrodes, the second term is due to the impedance of the material and the third term is due to C_g. Figure 2 is an impedance model for (1) that includes a resonant parallel *LCR* circuit, identical to that described in [7] for measurements performed with direct-contact electrodes and corresponds to the third term in (1). This term, additional to those attributable to electrodes and material, severely distorts the impedance measured at frequencies close to the characteristic frequency of the material, $\omega_c = (R_x C_x)^{-1}$. If in order to avoid that effect we measure at a lower frequency, $\omega << \omega_c$, the result is

$$Z_{HL}(j\omega)\big|_{\omega C_x R_x << 1} \approx R_x\left(1 + \frac{C_g}{C_e}\right) + \frac{1}{j\omega\dfrac{C_e}{2 + C_g/C_e}} \quad (2)$$

that shows that even at frequencies well below ω_c , both the real and the imaginary part of the result are affected by C_g/C_e. If this factor is not negligible with respect to 1, then the measured resistance, which will correspond to the two central *RC* networks in Fig. 2, will be larger than that of the material (Re $Z_{HL} > R_x$). Contrarily, $C_{HL} = (-\omega \mathrm{Im}\, Z_{HL})^{-1}$, due to the two capacitances in the left of Fig. 2, will be smaller than $C_e/2$ and the measured capacitance will be smaller than the actual electrode capacitance.

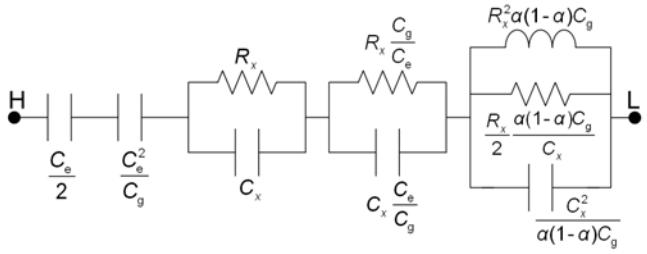

Fig. 2. Equivalent two-terminal impedance model for bipolar impedance measurements with capacitive electrodes.

Equation (2) also shows that measurements well below ω_c do not inform about C_x. If in order to estimate C_x we measure at frequencies much larger than ω_c, the result will be

$$Z_{HL}(j\omega)\big|_{\omega R_x C_x >> 1} \approx \frac{1}{j\omega\dfrac{C_e}{2 + C_g/C_e}} + \frac{1}{j\omega\dfrac{C_x}{1 + C_g/C_e + \alpha(1-\alpha)C_g/C_x}} \quad (3)$$

which is a purely capacitive impedance that includes the five capacitances in Fig. 2. Therefore, in addition to the contribution of electrode impedance, affected by C_g/C_e, the measurement of the material capacitance (C_x) is affected by C_g/C_e and by an additional factor $\alpha(1 - \alpha)C_g/C_x$ that depends on α, C_g and C_x itself. This nonlinear relationship between the measured capacitance and the actual material capacitance is the same found for galvanic electrodes [7]. If the first term of (3) is determined from the imaginary part of (2), and subtracted from (3), the resulting capacitance will be smaller than C_x and the deviation will depend on C_x itself.

3. EXPERIMENTAL RESULTS AND DISCUSSION

We measured Re Z_{HL} and Im Z_{HL} for two water samples inside a cell built from a 100 mL polypropylene syringe Omnifix® (B. Braun Melsungen AG), which respective external and internal diameters were 30,6 mm and 28,0 mm and 12 cm length. The capacitive electrodes were two 25 mm-wide copper strips wrapped around the syringe and with inner ends 50 mm apart (Fig. 3). The electrodes were connected to an impedance analyser (Agilent 4294A) by two 90 mm long, single-core silicone-rubber-insulated cables with 1 mm^2 cross section. The syringe was placed over a 305 mm × 227 mm copper plane grounded at the enclosure of the impedance analyser (Fig. 4). The cell was successively placed at three different heights above ground, $h = \{52, 8, 1{,}7\}$ mm in order to obtain three different C_g values $\{C_{g52} < C_{g8} < C_{g1,7}\}$. The frequency range of interest was from 1 kHz to 10 MHz but some results were displayed up to 100 MHz. The electrical conductivity of the two water samples used, measured with a Tetracon® 325 probe connected to a WTW conductivity meter model 340i were 0,01 dS/m (10 ± 1 µS/cm) and 1 dS/m (1000 ± 6 µS/cm), referred to 25,0 °C, and their relative permittivity was 78,3 [9]. The sample was at 22,0 °C so that the corrected conductivities and permittivity were 0,0094 dS/m, 0,94 dS/m and 79,4 [10] hence the characteristic frequency of the samples were f_c = 213 kHz and 21,3 MHz.

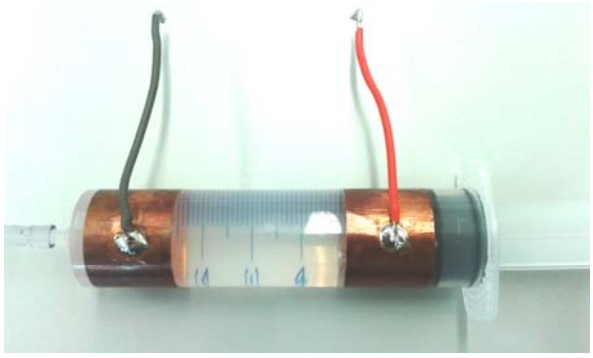

Fig. 3. Measurement cell with capacitive electrodes built from a polypropylene syringe and two copper rings.

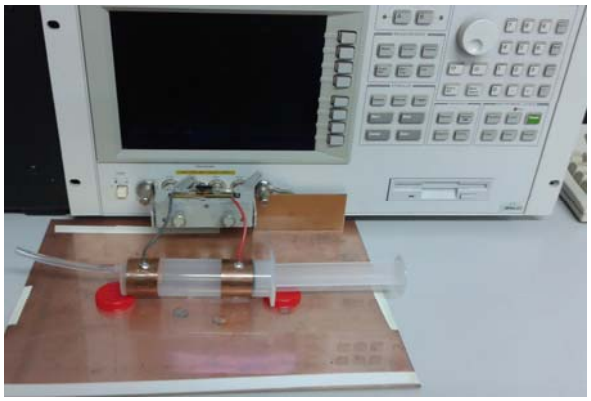

Fig. 4. Measurement setup with the cell placed over a ground plane and connected to the impedance analyser by single core cables.

Figure 5 shows that the measured real part of the impedance for the 0,01 dS/m sample was different for each cell height and increased for increasing C_g, as predicted by (2). At 15 kHz ($<< f_c$ = 213 kHz) Re Z_{HL} is flat, as expected, and Re Z_{HL} is 119 kΩ when h = 52 mm, 125 kΩ when h = 8 mm and 138 kΩ when h = 1,7 mm. At frequencies below about 5 kHz, Re Z_{HL} increases for decreasing frequencies whereas according to (2) it should remain constant. This suggests that maybe electrode resistance, in parallel with C_e, is not large enough to be neglected because C_e is very small. But polypropylene is known to have a very high insulation resistance. An alternative explanation could be a limited surface resistance of the syringe, which decreases if it becomes moist, which was easily verified by blowing into it.

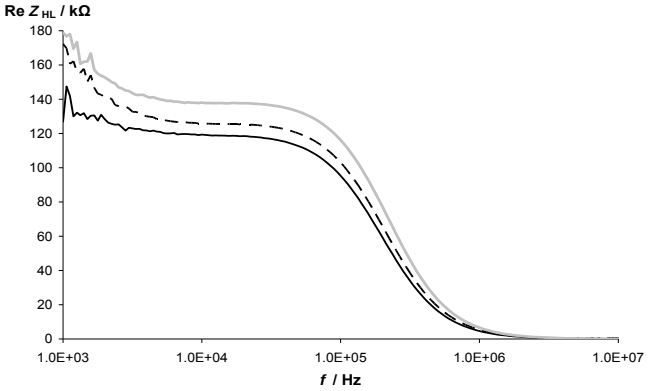

Fig. 5. Real part of Z_{HL} (0,01 dS/m) when the height of the cell above the ground plane was 52 mm (solid black line), 8 mm (dashed black line) and 1,7 mm (solid grey line).

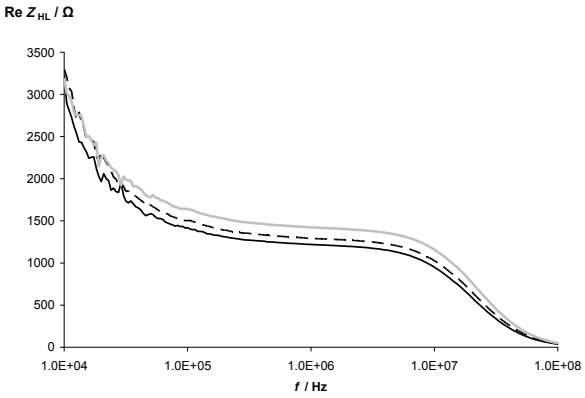

Fig. 6. Real part of Z_{HL} (1,0 dS/m) when the height of the cell above the ground plane was 52 mm (solid black line), 8 mm (dashed black line) and 1,7 mm (solid grey line).

For the 1,0 dS/m water sample, Fig. 6 shows that at 1 MHz ($<< f_c$ = 21,3 MHz) Re Z_{HL} was 1220 Ω when h = 52 mm, 1293 Ω when h = 8 mm and 1423 Ω when h = 1,7 mm, that is, about 100 times smaller than in Fig. 5, as expected because it was 100 times more conductive. But now no flat region can be easily identified because of the "low-frequency" increase due to the electrode/cell resistance unaccounted for in Fig. 1 and (2). In order to assess the influence of that resistance, the ground plane in Fig. 4 was removed and Re Z_{HL} was measured for the cell full of 1,0 dS/m water. At 10 kHz, the result was 2,6 kΩ, which increased to 4,8 kΩ when blowing into the cell. At 100 kHz the result was 1497 Ω, which increased to 1655 Ω when blowing into the cell.

The results for C_{HL} from 1 kHz to 10 MHz for the first water sample (0,01 dS/m) are shown in Fig. 7. At low frequencies, C_{HL} corresponds to the imaginary part of (2) hence depends mainly on electrode capacitance C_e but it is affected by C_g/C_e in such a way that instead of obtaining $C_e/2$, the apparent capacitance decreases for increasing C_g/C_e ratio. In Fig. 7, at 1 kHz C_{HL} is 16,9 pF when h = 52 mm, 16,3 pF when h = 8 mm and 15,4 pF when h = 1,7 mm, which corroborates that dependence. That is, reducing h by 85 % when it is large (52 mm), decreases C_{HL} only by 3,5 %, but reducing h by 79 % when it is smaller (8 mm) reduces C_{HL} by 5,5 %, which suggests that C_g/C_e, hence C_g, is not proportional to h. Instead, C_g is proportionally larger for smaller h, as it could be expected because of the far smaller area of the sample as compared to that of the ground plane. The results for 1,0 dS/m water at 10 kHz were about the same: C_{HL} is 17,0 pF when h = 52 mm, 16,3 pF when h = 8 mm and 15,4 pF when h = 1,7 mm. Therefore, C_e and C_g do not depend on material conductivity, whereas C_e for direct-contact electrodes does.

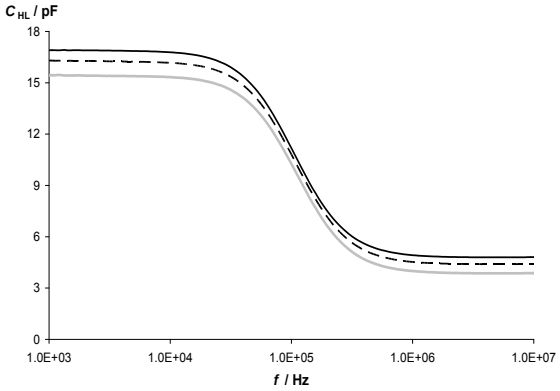

Fig. 7. C_{HL} measured for the cell with the first water sample (0,01 dS/m) at 52 mm (solid black line), 8 mm (dashed black line) and 1,7 mm (solid grey line) above the ground plane.

At frequencies much higher than f_c, (3) applies and C_{HL} corresponds to electrode capacitance "modified" by C_g/C_e, in series with material capacitance C_x, also modified by C_g/C_x in addition to C_g/C_e. In both cases, the modification is in the sense of a decreasing measured capacitance for increasing C_g/C_x and C_g/C_e ratios. In Fig. 7, at 10 MHz C_{HL} is 4,8 pF when h = 52 mm, 4,4 pF when h = 8 mm and 3,9 pF when h = 1,7 mm. Therefore, the decrease of C_{HL} with increasing C_g is verified: 85 % reduction in h (from 52 to 8 mm) results in 8 % reduction in C_{HL}, and 79 % reduction in h (from 8 to 1,7 mm) reduces C_{HL} by 11 %.

C_g can be calculated from Im Z_{HL} in (2) provided C_e was known. In order to determine C_e, we measured the cell capacitance using a battery supplied RLC meter (Agilent U1733C). Battery supply implies negligible C_g because of the isolation capacitance between the meter and earth ground. At 10 kHz, for the second water sample we obtained $C_e \approx (34{,}9 \pm 0{,}1)$ pF, which is compatible with C_{HL} values in Fig. 7. Regrettably, the limited resolution of this low-cost instrument cannot produce stable readings for the real part of the impedance of the cell, but in (2) we can estimate C_g from Im Z_{HL} and then R_x from Re Z_{HL}. In Table 1, relative R_x

deviations in excess of 2 % due to C_g can be easily observed. The decrease of C_g with increasing h, hence the reduction of its effect, is faster for small h than for large h, as already deducted in Figs. 5, 6 and 7. However, this does not mean that C_g becomes irrelevant for h values about a few centimetres because the enclosure of the impedance analyser is grounded hence the material being measured is also capacitively coupled to ground through the instrument. Attempts to reduce this capacitive coupling by increasing the length of the connecting wires would fail because of the increased parasitic inductance of that connection.

Table 1. C_g calculated from Im Z_{HL} and R_x from Re Z_{HL} in (2) after C_e (= 34,9 pF) has been measured with a battery-supplied RLC meter.

h (mm)	52	8	1,7
$1 + C_g/C_e$	1,065	1,141	1,266
C_g (pF)	2,3	4,9	9,3
R_x (kΩ) [0,01 dS/m]	111,7	109,5	109,0
R_x (Ω) [1,00 dS/m]	1145,4	1133,1	1123,8

The approach used for R_x cannot be applied to estimate C_x because, in order to that, in (3) we need $\alpha(1 - \alpha)$ in addition to C_e and C_g. Further, (3) applies only when measuring at $f >> f_c$, which for low-conductivity samples would mean frequencies well above, say, 10 MHz because f_c = 213 kHz and we need to measure in the flat region of the C_{HL} curve. Then the distance between electrodes would be comparable to $\lambda/126$ and wave propagation effects would appear [11]. For example, at 10 MHz, $\lambda/126 \approx 2{,}6$ cm and electrode separation in the cell in Fig. 3 is just 5 cm. If the electrodes were closer, the capacitance between them in the absence of any material (C_{hl}) would be relevant and the model in Fig. 1 would not apply. For high-conductivity materials, the measurement frequency should be even higher.

Therefore, dielectric measurements with capacitive electrodes must be performed at too high frequencies for lumped-parameter models to hold. Measurements performed with direct-contact electrodes have been demonstrated to be also affected by C_g/C_e, but C_e for direct-contact electrodes is orders of magnitude larger than for capacitive electrodes (tens of picofarads) hence those effects are negligible at low frequencies and, in some cases, even at frequencies close to the characteristic frequency of the material.

4. CONCLUSIONS

The measurement of water impedance by using two capacitive electrodes with a grounded instrument based on an auto-balancing bridge method is affected by the stray capacitance C_g from the volume of the sample to ground. The real part of the measured impedance Re Z_{HL} increases and the measured capacitance C_{HL} decreases for increasing C_g. At low frequencies relative to the characteristic frequency of the material, $\omega_c = (R_x C_x)^{-1}$, these effects depend on C_g/C_e and imply an overestimation of R_x and underestimation of electrode capacitance C_e.

C_x cannot be determined form low frequency measurements. Measurements at frequencies close to ω_c are also strongly affected by C_g and cannot help in determining C_x either. At high frequencies relative to ω_c the decrease in C_{HL} depends on C_x but also on $C_g/C_e + \alpha(1 - \alpha)C_g/C_x$ so that there is an underestimation of both C_e and material capacitance C_x. C_g can be reduced by increasing the distance between the cell with the sample material and nearby grounded objects. Nevertheless, distancing too much the cell from the grounded enclosure of impedance analyser would require long cables which stray inductance would affect high frequency measurements.

For materials which characteristic frequency exceeds about 100 kHz, C_x should be measured at frequencies whose wavelength would be comparable to electrode separation, which would lead to wave propagation effects. Closer electrodes would reduce that effect but then inter-electrode capacitance could limit the maximal measurement frequency.

ACKNOWLEDGMENTS

The authors would like to thank the Castelldefels School of Telecommunications and Aerospace Engineering (EETAC, BarcelonaTech - UPC) for its research facilities and Mr. F. López for his technical support.

REFERENCES

[1] W. Göpel, J. Hesse and J. N. Zemel, *Sensors. A Comprehensive Survey*, vol. 2, VCH Verlagsgesellschaft mbH, Weinheim, Germany, 1991, Ch. 7, Sec. 3, pp. 314-332.

[2] M. C. Hofmann, D. Ellersiek, F. Kensy, J. Büchs, W. Mokwa and U. Schnakenberg, "Galvanic decoupled sensor for monitoring biomass concentration during fermentation processes," *Sens. Actuators B*, vol. 111, pp. 370-375, November 2005.

[3] M. Ballico, "A technique for in situ measurement of the conductivity of water in 'triple point of water' cells," *Meas. Sci. Technol*., vol. 10, no. 7, pp. L33-L36, July 1999.

[4] D. Strazza, M. Demori, V. Ferrari, and P. Poesio, "Capacitance sensor for hold-up measurement in high-viscous-oil/conductive-water core-annular flows," *Flow Meas. Instrum.*, vol. 22, no. 5, pp. 360-369, October 2011.

[5] F. Opekar, P. Tůma and K. Štulík, "Contactless Impedance Sensors and Their Application to Flow Measurements," Sensors, vol. 13, no. 3, pp. 2786-2801, February 2013.

[6] B. Gaš, J. Zuska, P. Coufal and T. van de Goor, "Optimization of the high-frequency contactless conductivity detector for capillary electrophoresis," *Electrophoresis*, vol. 23, no. 20, pp. 3520-3527, October 2002.

[7] C. Aliau-Bonet and R. Pallas-Areny, "Effects of Stray Capacitance to Ground in Bipolar Material Impedance Measurements Based on Direct-Contact Electrodes," *IEEE Trans. Instrum. Meas*., vol. 63, no. 10, pp. 2414-2421, October 2014.

[8] *The Impedance Measurement Handbook, A Guide to Measurement Technology and Techniques*, Agilent Technologies Co. Ltd., 2006. Available: http://cp.literature.agilent.com/litweb/pdf/5950-3000.pdf

[9] A. R. Von Hippel, *Dielectric materials and applications*, Cambridge MA: MIT Press, 1954

[10] A. Stogryn, "Equations for calculating the dielectric constant of saline water," *IEEE Trans. Microwave Tech.*, vol. MTT-19, pp. 733–736, Aug.1971.

[11] A. Straub, "Boundary element modelling of a capacitive probe for in situ soil moisture characterization," *IEEE Trans. Geosci. Remote Sens.*, vol. 32, no 2, pp. 261-266, Mar. 1994.